Catal Lett (2008) 125:283–288
DOI 10.1007/s10562-008-9560-z

Combined H_2O and CO_2 Reforming of Methane Over Ni–Ce–ZrO_2 Catalysts for Gas to Liquids (GTL)

Hyun-Seog Roh · Kee Young Koo · U. D. Joshi · Wang Lai Yoon

Received: 2 June 2008 / Accepted: 17 June 2008 / Published online: 18 July 2008

Abstract Ni–Ce–ZrO_2 catalysts with various CeO_2/ZrO_2 ratios have been prepared by co-precipitation method and applied for combined steam and carbon dioxide reforming of methane (CSCRM) to produce synthesis gas ($H_2/CO = 2$) for gas to liquid (GTL) process. 15% Ni–$Ce_{0.8}Zr_{0.2}O_2$ exhibits the highest activity as well as stability in CSCRM due to finely dispersed NiO with intimate contact with support and high oxygen storage capacity.

Keywords Synthesis gas · Combined reforming · Methane · Ni · Ce–ZrO_2 · Catalyst

1 Introduction

Gas to liquids (GTL) technology attracts significant research interest due to high oil price. GTL technology consists of synthesis gas production, Fischer–Tropsch (FT) synthesis and product work-up. The synthesis gas preparation section is an important part of the entire GTL complex because it is the most expensive of the three process sections and is responsible for the largest part of the energy conversion in the plant. Therefore, the design of the synthesis gas preparation unit is critical for the economics of a GTL project [1]. Commercially, synthesis gas has been produced from steam reforming of methane (SRM) [2–4]. However, SRM by itself is not the preferred technology to produce synthesis gas for the GTL applications because the H_2/CO ratio from steam reforming is higher than 3, which is not suitable for the FT synthesis. As an alternative, catalytic partial oxidation of methane (POM) to H_2 and CO has advantages such as mild exothermicity, suitable H_2/CO ratio for the FT syntheses, and very short residence time [5–9]. However, POM has disadvantages such as explosion danger and difficulty in controlling the operation. Due to these demerits, POM has not been commercialized even though it is estimated to be more economical than SRM [10].

As an alternative, combined steam and carbon dioxide reforming of methane (CSCRM), where steam is partially substituted by carbon dioxide, can be employed to produce synthesis gas with flexible H_2/CO ratio [11–14]. CSCRM offers great advantage to adjust H_2/CO ratio in the product synthesis gas to meet the requirements of downstream chemical synthesis such as FT synthesis [11]. By co-feeding steam and carbon dioxide, the H_2/CO ratio can be controlled by changing the $H_2O/CO_2/CH_4$ ratio in the reaction feed [12].

It is known that supported Ni catalysts easily deactivate due to carbon formation in carbon dioxide reforming of methane (CRM) as well as in CSCRM [11, 12]. Thus, it is an important topic to develop active and stable catalysts in CSCRM. Recently, it has been reported that the Ni catalyst supported by small nanoparticles of ZrO_2, MgO, and Ce–ZrO_2 could be highly active and stable for CRM [11, 15–17]. Very recently, Roh et al. reported that Ni/MgO–Al_2O_3 exhibited high activity as well as stability in CSCRM due to enhanced steam adsorption, basic property, fine dispersion, and strong Ni to support interaction [12]. As a

H.-S. Roh (✉)
Department of Environmental Engineering, Yonsei University,
234 Maeji, Heungeop, Wonju, Gangwon-do 220-710,
South Korea
e-mail: hsroh@yonsei.ac.kr

K. Y. Koo · U. D. Joshi · W. L. Yoon (✉)
Strategic Technologies Research Division, Korea Institute
of Energy Research (KIER), 71-2 Jang-dong, Yuseong,
Daejeon 305-343, South Korea
e-mail: wlyoon@kier.re.kr

consequence, the role of support is very important to achieve high activity as well as stability in CSCRM.

Researchers have been interested in Ce_{1-x}–Zr_xO_2 catalytic systems [18]. It has been reported that the addition of ZrO_2 to CeO_2 leads to improvements in oxygen storage capacity of CeO_2, redox property, thermal stability, and promotion of metal dispersion due to the partial substitution of Ce^{4+} with Zr^{4+} in the lattice of CeO_2 resulting in solid solution formation [18–20]. As a result, the Ce_{1-x}–Zr_xO_2 system has been considered as a promising support material in nickel based catalyst systems [21–23]. Lercher et al. [24] reported that Pt/ZrO_2 showed excellent performance in CDR. Li et al. [25, 26] reported that Ni/ZrO_2 catalysts with more than 10 wt% Ni loading showed high activity in CDR under diluted reaction conditions. Previously, Ni catalysts supported on a tetragonal $Ce_{0.2}$–$Zr_{0.8}O_2$ prepared by the molten salt method were applied to SRM [3, 27], POM [8, 28], and oxy-SRM (OSRM) [27, 28]. Montoya et al. [29] applied Ni supported on a tetragonal CeO_2–ZrO_2 support for the CDR reaction. Roh et al. [30, 31] reported that Rh/Ce–ZrO_2 was highly active and selective in ethanol steam reforming. Jun and co-workers reported that a co-precipitation method was highly effective method to prepare Ni–Ce–ZrO_2 catalyst for CRM [16, 17, 32].

In this study, co-precipitated Ni–Ce–ZrO_2 catalysts with various CeO_2/ZrO_2 ratios have been prepared and applied for CSCRM to achieve a H_2/CO ratio of 2, which is suitable for the FT synthesis. The objective of this study was to optimize the CeO_2/ZrO_2 ratio in CSCRM for the GTL process. We report here that 15%Ni–$Ce_{0.8}$–$Zr_{0.2}O_2$ catalyst exhibits the highest activity as well as stability in CSCRM due to the beneficial effect of $Ce_{0.8}$–$Zr_{0.2}O_2$ and co-precipitation method.

2 Experimental

15%Ni–Ce–ZrO_2 with various Ce/Zr ratios were prepared by a co-precipitation method. Stoichiometric quantities of zirconyl nitrate solution (20 wt% ZrO_2 basis, MEL Chemicals), Ce-nitrate (99.9%, Aldrich), and Ni-nitrate (97%, Junsei Chemicals) were combined in distilled water. To this solution 10% KOH solution was added drop-wise at 80 °C to attain a pH of 10.5. The precipitate was digested at 80 °C for 3 days. After that, it was washed with distilled water several times and then air-dried for 48 h followed by drying at 110 °C for 6 h. The catalysts were calcined at 800 °C for 6 h in air. Commercial 10%Ni/α-Al_2O_3 and 2%Ru/α-Al_2O_3 catalysts were employed as references in CSCRM.

The BET surface areas were measured by nitrogen adsorption at −196 °C using a Micromeritics (ASAP-2400) surface area measurement apparatus. The XRD patterns were recorded using a Rigaku D/MAX-IIIC diffractometer (Ni filtered Cu-Kα radiation, 40 kV, 50 mA). The crystallite size of NiO and support in prepared catalysts was estimated using the Scherrer equation [21]. H_2-chemisorption was conducted in ASAP 2010 (Micromeritics). The calcined catalyst sample (about 0.2 g) was reduced at 800 °C for 1 h in H_2 flow and analyzed at 50 °C. Each point was measured after 5 min stabilization. From the chemisorbed amount, the Ni surface area was calculated by assuming the adsorption stoichiometry of one hydrogen atom per nickel surface atom ($H/Ni_s = 1$).

Activity tests were carried out at 800 °C under atmospheric pressure in a fixed-bed micro-tubular quartz reactor with an inner diameter of 4 mm. The catalyst charge was 10 mg, and $MgAl_2O_4$ was used as a catalyst diluent. A thermocouple was inserted into the catalyst bed to measure the reaction temperature. Prior to each catalytic measurement, the catalyst was reduced in 10% H_2/N_2 at 700 °C for 1 h. The reactant gas stream consisted of H_2O, CO_2, and CH_4. The feed $H_2O/CO_2/CH_4/N_2$ ratio was fixed at 0.8/0.4/1.0/1.0 to get the product H_2/CO ratio of 2. N_2 was employed to calculate CH_4 conversion. A space velocity of 265,000 cm^3 gas fed/g_{cat}-h was used to screen the catalysts in this study, unless otherwise stated. Water was fed using a syringe pump and was vaporized at 150 °C upstream of the reactor. The reformate was chilled, passed through a trap to condensate residual water, and then flowed to the on-line gas chromatograph (HP 6890N).

3 Results and Discussion

3.1 Catalyst Characterization

Table 1 summarizes the characteristics of the commercial 10%Ni/α-Al_2O_3 and 2%Ru/α-Al_2O_3 catalysts. The BET surface areas of both catalysts are less than 6 m^2/g, indicating that the support is α-alumina. Ru dispersion is 2.4% and Ni dispersion is 0.8%, respectively. Figure 1 shows XRD patterns of the commercial 10%Ni/α-Al_2O_3 and 2%Ru/α-Al_2O_3 catalysts. It is obvious that both catalysts have characteristic peaks of α-Al_2O_3 phase. In the case of 10%Ni/α-Al_2O_3 catalyst, NiO peak can be seen. The calculated NiO crystallite size is 25 nm. For 2%Ru/α-Al_2O_3

Table 1 Characteristics of 10%Ni/α-Al_2O_3 and 2%Ru/α-Al_2O_3 catalysts

Catalyst	Active component	Surface area (m^2/g)	Metal dispersion (%)
Ni/Al_2O_3	10 wt% Ni	3.6	0.8
Ru/Al_2O_3	2 wt% Ru	5.9	2.4

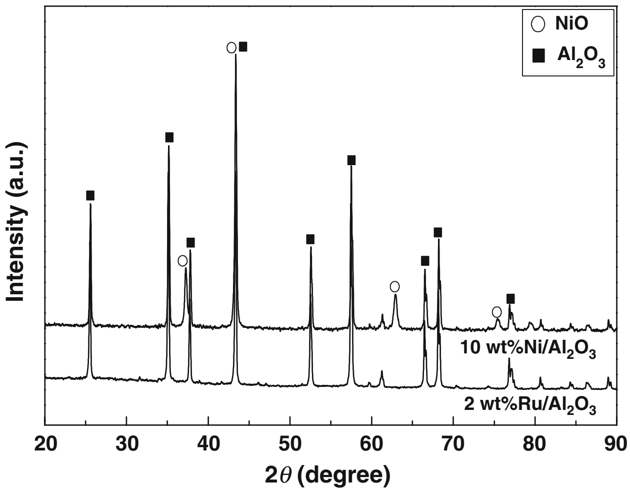

Fig. 1 XRD patterns of 10%Ni/α-Al_2O_3 and 2%Ru/α-Al_2O_3 catalysts

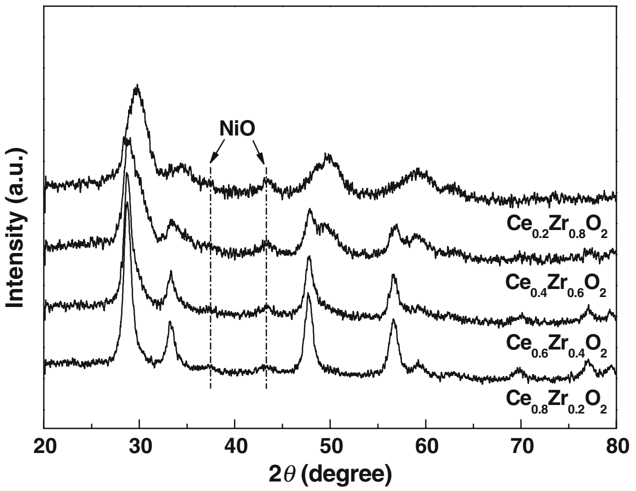

Fig. 2 XRD patterns of Ni–Ce–ZrO_2 catalysts with various Ce/Zr ratios

catalyst, Ru peak cannot be measured because of low Ru content.

Table 2 summarizes the characteristics of Ni–Ce–ZrO_2 catalysts with various Ce/Zr ratios. Among the catalysts, Ni–$Ce_{0.8}$–$Zr_{0.2}O_2$ catalyst shows the highest BET surface area and the highest Ni dispersion. It is reported that cubic $Ce_{0.8}$–$Zr_{0.2}O_2$ supported Ni catalyst shows the highest dispersion [17]. However, it is very rare case that Ni–$Ce_{0.8}$–$Zr_{0.2}O_2$ catalyst calcined at 800 °C for 6 h has BET surface area of 97 m^2/g. Jun and co-workers reported that BET surface area of 80 m^2/g was obtained after calcination at 800 °C for 6 h with the same composition (15% Ni–$Ce_{0.8}$–$Zr_{0.2}O_2$) [32]. Thus, the catalyst used in this study has been prepared well with high surface area, which is important to get high dispersion of metal and to achieve high activity in CSCRM.

Figure 2 depicts XRD patterns of Ni–Ce–ZrO_2 catalysts with various Ce/Zr ratios. Ni–$Ce_{0.8}$–$Zr_{0.2}O_2$ catalyst shows the characteristic peaks corresponding to cubic $Ce_{0.8}$–$Zr_{0.2}O_2$ solid solution [32].The observed NiO peaks are too broad to calculate the crystallite size of NiO. This indicates that NiO is well incorporated into $Ce_{0.8}$–$Zr_{0.2}O_2$ solid solution. Like Ni–$Ce_{0.8}Zr_{0.2}O_2$ catalyst, Ni–$Ce_{0.6}Zr_{0.4}O_2$ catalyst has cubic phase, while Ni-$Ce_{0.2}Zr_{0.8}O_2$ illustrates tetragonal phase [17]. In the case of Ni–$Ce_{0.4}Zr_{0.6}O_2$, the XRD pattern shows the transition state from cubic to tetragonal but close to cubic phase. As Ce/Zr ratio increases, the NiO peaks become sharp. In the case of Ni–$Ce_{0.2}$–$Zr_{0.8}O_2$ catalyst, the crystallite size of NiO calculated by Scherrer equation is found to be 7 nm. Thus, it has been confirmed that Ni–$Ce_{0.8}$–$Zr_{0.2}O_2$ forms solid solution without segregation of NiO. This also indicates that the interaction between Ni and $Ce_{0.8}$–$Zr_{0.2}O_2$ will be stronger.

Table 2 Characteristics of Ni–Ce–ZrO_2 catalysts with various Ce/Zr ratios

Catalyst	Surface area (m^2/g)	NiO size (nm)	Support size (nm)	Metal dispersion (%)
Ni–$Ce_{0.8}$–$Zr_{0.2}O_2$	97	<3	9	2.16
Ni–$Ce_{0.6}$–$Zr_{0.4}O_2$	90	<3	8	1.59
Ni–$Ce_{0.4}$–$Zr_{0.6}O_2$	83	<3	4	0.97
Ni–$Ce_{0.2}$–$Zr_{0.8}O_2$	86	7	3	1.04

It is known that $Ce_{0.8}Zr_{0.2}O_2$ with cubic phase has higher oxygen storage capacity than $Ce_{0.2}Zr_{0.8}O_2$ with tetragonal phase [17]. Therefore, it can be concluded that oxygen ion vacancies in the cubic $Ce_{0.8}Zr_{0.2}O_2$ support have beneficial effects on catalytic stability due to the enhanced oxygen transfer during the CSCRM reaction, resulting in keeping the Ni surface from carbon formation.

3.2 Reaction Results

Previously, the $H_2O/CO_2/CH_4$ ratio in the reaction feed was systematically changed to adjust H_2/CO ratio in the product synthesis gas to be suitable for FT in GTL. According to the previous results, the product H_2/CO ratio of 2 was achieved with the $H_2O/CO_2/CH_4$ ratio of 0.8/0.4/1.0 in the feed stream [12].

Figure 3 shows CH_4 conversion with time on stream over commercial 10%Ni/α-Al_2O_3 and 2%Ru/α-Al_2O_3 catalysts. It is clear that both catalysts deactivated with time on stream. Especially, commercial Ni/α-alumina catalyst rapidly deactivated with time on stream due to carbon formation. After the reaction, serious coke formation could be seen along the reactor. In the case of commercial Ru/α-alumina catalyst, it relatively slowly deactivated with time on stream even though Ru is precious metal. These results suggest that both catalysts were not suitable for CSCRM.

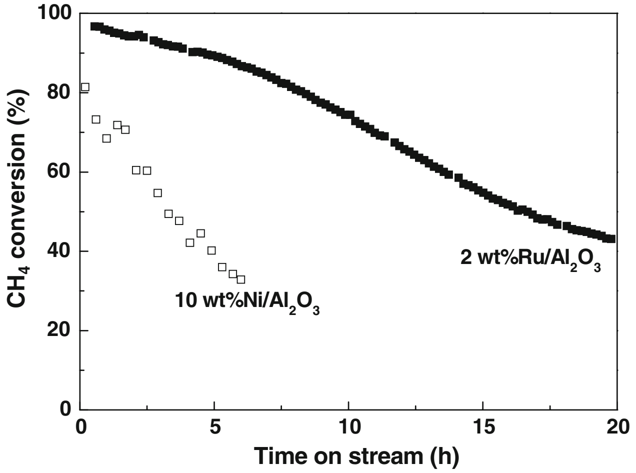

Fig. 3 Reaction data over 10%Ni/α-Al$_2$O$_3$ and 2%Ru/α-Al$_2$O$_3$ catalysts

In addition, Ni/MgAl$_2$O$_4$ was reported to suffer from coke formation in CSCRM [12]. This is due to the fact that the commercial catalysts have been optimized in SRM with excess steam to methane ratio. Commercially, steam to methane ratio is usually more than 3 to avoid carbon formation [2, 3]. With stoichiometric steam to methane ratio ($H_2O/CH_4 = 1.0$) in SRM, the commercial catalyst was reported to deactivate with time on stream [4]. In CSCRM, the reaction condition used in this study, namely $(H_2O + CO_2)/CH_4 = 1.2$, is very severe condition. Thus, it is necessary to develop new catalyst for CSCRM in GTL.

Figure 4 presents CH$_4$ conversion with time on stream over Ni–Ce–ZrO$_2$ catalysts with various Ce/Zr ratios. It is obvious that Ni–Ce$_{0.8}$–Zr$_{0.2}$O$_2$ catalyst exhibited the highest CH$_4$ conversion as well as stability with time on stream in CSCRM. On the contrary, the other catalysts deactivated with time on stream. The degree of catalyst deactivation was strongly dependent upon the Ce/Zr ratio in Ni–Ce–ZrO$_2$ catalysts. In the case of Ni–Ce$_{0.2}$–Zr$_{0.8}$O$_2$ catalyst, the rate of catalyst deactivation was fast among the catalysts. The rate of catalyst deactivation follows the order: Ni–Ce$_{0.2}$–Zr$_{0.8}$O$_2$ > Ni–Ce$_{0.4}$–Zr$_{0.6}$O$_2$ > Ni–Ce$_{0.6}$–Zr$_{0.4}$O$_2$. It should be noted that Ni–Ce$_{0.8}$–Zr$_{0.2}$O$_2$ catalyst showed relatively stable activity for 20 h. Thus, it is most likely that high activity and stability is closely related with NiO crystallite size. According to the XRD analyses, Ni–Ce$_{0.2}$–Zr$_{0.8}$O$_2$ has the largest NiO crystallite size (7 nm). Moreover, NiO peak is most broad over Ni–Ce$_{0.8}$–Zr$_{0.2}$O$_2$ (Fig. 2). As a result, it is expected that the interaction between Ni and support will be the strongest in Ni–Ce$_{0.8}$–Zr$_{0.2}$O$_2$. If that is the case, the mobile oxygen species can be effectively transferred from the support to Ni during CSCRM, resulting in preventing coke formation. This is in good agreement with the previous results [16, 17]. It has been reported that nano-sized NiO has strong coke resistance in methane reforming reactions [17]. It is also reported that mobile oxygen species is effectively supplied from support to Ni over Ni–Ce–ZrO$_2$ catalysts due to strong metal to support interaction (SMSI) [33].

Figure 5 shows CO$_2$ conversion with time on stream over Ni–Ce–ZrO$_2$ catalysts with various Ce/Zr ratios. Initial CO$_2$ conversion is about 20% lower than CH$_4$ conversion. This is due to the fact that feed $(H_2O + CO_2)/CH_4$ ratio was fixed at 1.2, which is slightly higher than stoichiometric feed ratio. In addition, H$_2$O is more reactive than CO$_2$ as an oxygen source in CSCRM. By the way, the general trend of CO$_2$ conversion with time on stream is similar to that of CH$_4$ conversion with time on stream.

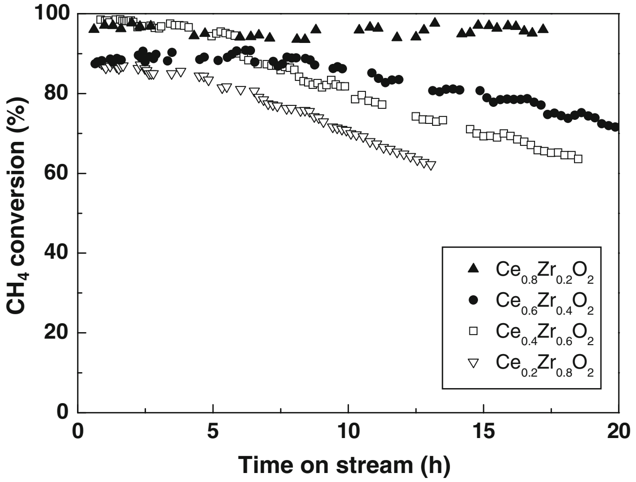

Fig. 4 CH$_4$ conversion over Ni–Ce–ZrO$_2$ catalysts with various Ce/Zr ratios (reaction conditions: T = 800 °C, GHSV = 265,000 mL/h g$_{cat}$)

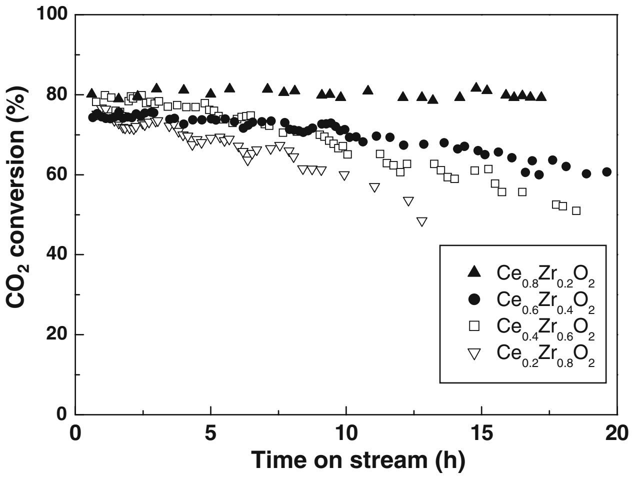

Fig. 5 CO$_2$ conversion over Ni–Ce–ZrO$_2$ catalysts with various Ce/Zr ratios (reaction conditions: T = 800 °C, GHSV = 265,000 mL/h g$_{cat}$)

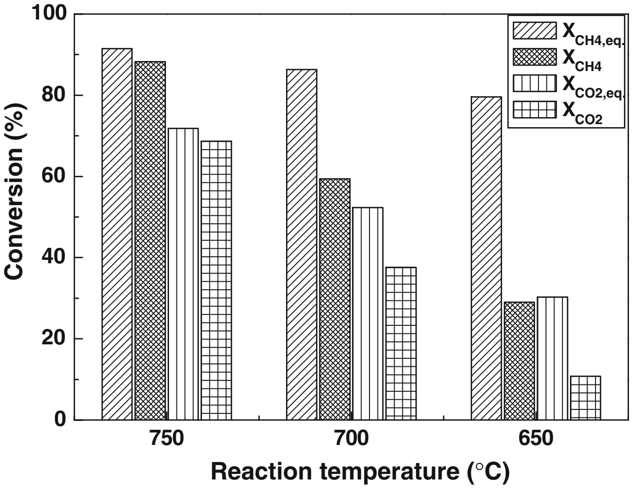

Fig. 6 Conversion vs. reaction temperature over Ni–$Ce_{0.8}Zr_{0.2}O_2$ (GHSV = 1,060,000 mL/h g_{cat}; ▨: Equilibrium CH_4 conversion, ▩: Experimental CH_4 conversion, ▥: Equilibrium CO_2 conversion, ▦: Experimental CO_2 conversion)

Clearly, Ni–$Ce_{0.8}$–$Zr_{0.2}O_2$ catalyst showed the highest CO_2 conversion with stability in CSCRM. Like the results on CH_4 conversion with time on stream, the other catalysts deactivated with time on stream. The rate of catalyst deactivation follows the order: Ni–$Ce_{0.2}$–$Zr_{0.8}O_2$ > Ni–$Ce_{0.4}$–$Zr_{0.6}O_2$ > Ni–$Ce_{0.6}$–$Zr_{0.4}O_2$.

To see the effect of reaction temperature on CH_4 and CO_2 conversion, the reaction temperature was changed from 750 °C to 650 °C at the GHSV of 1,060,000 mL/h g_{cat}. Because Ni–$Ce_{0.8}$–$Zr_{0.2}O_2$ catalyst showed almost equilibrium CH_4 conversion (97%) and CO_2 conversion (79%) at 800 °C and 265,000 mL/h g_{cat}, the GHSV was four times increased to avoid equilibrium limited condition. Figure 6 shows CH_4 and CO_2 conversion with reaction temperature over Ni–$Ce_{0.8}$–$Zr_{0.2}O_2$ catalyst. Both CH_4 and CO_2 conversion decreased with decreasing the reaction temperature from 750 °C to 650 °C because CSCRM is the highly endothermic reaction. The catalyst showed 88% CH_4 conversion and 69% CO_2 conversion, which are close to equilibrium CH_4 conversion (92%) and CO_2 conversion (72%) at 750 °C. It should be noted that it is very rare case that the supported Ni catalyst exhibited very high CH_4 and CO_2 conversion even at the GHSV of 1,060,000 mL/h g_{cat}. This suggests that Ni–$Ce_{0.8}$–$Zr_{0.2}O_2$ catalyst is extremely active in CSCRM. As a consequence, this catalyst will be a promising candidate catalyst for CSCRM in GTL.

To check the H_2/CO ratio in the synthesis gas, H_2/CO ratios with reaction temperature over Ni–$Ce_{0.8}$–$Zr_{0.2}O_2$ catalyst are summarized in Table 3. In the range of 700–800 °C the H_2/CO ratio is about 1.9–2.0, which is suitable for the FT synthesis in GTL. Thus, it is also confirmed that CSCRM over this catalyst is effective for GTL.

Table 3 H_2/CO ratios with reaction temperature over Ni–$Ce_{0.8}Zr_{0.2}O_2$

Temperature (°C)	650	700	750	800
H_2/CO	2.3	2.0	1.9	1.9

To see the effect of GHSV on CH_4 conversion, the GHSV was changed from 265,000 to 1,060,000 mL/h g_{cat} over Ni–$Ce_{0.8}$–$Zr_{0.2}O_2$ catalyst at 650 °C (Fig. 7). At the GHSV of 265,000 mL/h g_{cat}, the CH_4 conversion was similar to the equilibrium value (80%). It means that the catalyst is very active even at 650 °C. The CH_4 conversion decreased with increasing GHSV.

Table 4 summarizes the CH_4 conversion (X_{CH_4}) over supported Ni catalysts, which exhibited good catalytic performance in CSCRM in the literature. For comparison, the GHSV was calculated based on CH_4 only among the reactants. To our knowledge, Ni–$Ce_{0.8}$–$Zr_{0.2}O_2$ catalyst exhibited the best performance among the catalysts reported in the literature for CSCRM [11, 12, 34]. Thus, we believe that Ni–$Ce_{0.8}$–$Zr_{0.2}O_2$ catalyst is the promising candidate catalyst for CSCRM.

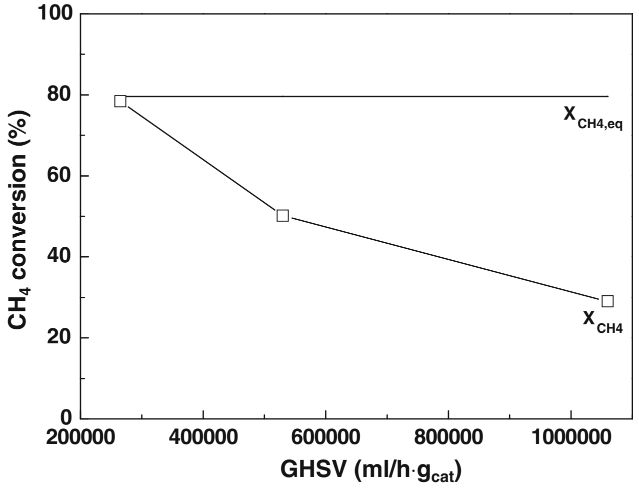

Fig. 7 CH_4 conversion vs. GHSV over Ni–$Ce_{0.8}Zr_{0.2}O_2$ (T = 650 °C) ($X_{CH_4,eq}$ = solid line, X_{CH_4} = with legends)

Table 4 Comparison of the CH_4 conversion in CSCRM

Catalyst	$GHSV_{CH_4}$ (mL/h g_{cat})	X_{CH_4} (%)	References
Ni–$Ce_{0.8}$–$Zr_{0.2}O_2$	82,800	97	This work
Ni/MgO–Al_2O_3	82,800	93	[12]
Ni/ZrO_2	12,000	89	[11]
Rh/MgO	118,000	45	[34]

All the reactions were carried out at 800 °C

4 Conclusions

The cubic Ni–$Ce_{0.8}Zr_{0.2}O_2$ exhibits the highest activity as well as stability in CSCRM due to finely dispersed NiO and nano-crystalline nature of $Ce_{0.8}Zr_{0.2}O_2$ with strong metal to support interaction and high oxygen storage capacity, resulting in increasing availability of surface oxygen, which prevents carbon formation during the reaction. The cubic Ni–$Ce_{0.8}Zr_{0.2}O_2$ catalyst can be a promising candidate catalyst for synthesis gas preparation for GTL.

Acknowledgments The authors would like to acknowledge the financial support of KEMCO and GTL Technology Development Consortium (Korea National Oil Corp., Daelim Industrial Co., LTD, Doosan Mecatec Co., LTD, Hyundai Engineering Co. LTD and SK Energy Co. LTD) under "Energy & Resources Technology Development Programs" of the Ministry of Knowledge Economy, Republic of Korea.

References

1. Aasberg-Petersen K, Christensen TS, Dybkjaer I, Sehested J, Ostberg M, Coertzen RM, Keyser MJ, Steynberg AP (2004) Stud Surf Sci Catal 152:258
2. Rostrup-Nielsen JR (1984) In: Anderson JR, Boudart M (eds) Catalysis, science and technology, vol 5. Springer, Berlin, p 1
3. Roh H-S, Jun K-W, Dong W-S, Chang J-S, Park S-E, Joe Y-I (2002) J Mol Catal A 181:137
4. Roh H-S, Jun K-W, Park S-E (2003) Appl Catal A 251:275
5. Tsang SC, Claridge JB, Green MLH (1995) Catal Today 23:3
6. Ashcroft AT, Cheetham AK, Foord JS, Green MLH, Grey CP, Murrell AJ, Vernon PDF (1990) Nature 344:319
7. Choudhary VR, Mamman AS, Sansare D (1992) Angew Chem Int Ed Engl 31:1189
8. Roh H-S, Dong W-S, Jun K-W, Park S-E (2001) Chem Lett 88
9. Roh H-S, Jun K-W, Dong W-S, Park S-E, Joe Y-I (2001) Chem Lett 666
10. Peña MA, Gómez JP, Fierro JLG (1996) Appl Catal A 144:7
11. Zhang Q-H, Li Y, Xu B-Q (2004) Catal Today 98:601
12. Roh H-S, Koo KY, Jeong JH, Seo YT, Seo DJ, Seo Y-S, Yoon WL, Park SB (2007) Catal Lett 117:85
13. Koo KY, Roh H-S, Seo YT, Seo DJ, Yoon WL, Park SB (2008) Appl Catal A 340:183
14. Koo KY, Roh H-S, Seo YT, Seo DJ, Yoon WL, Park SB (2008) Int J Hydrogen Energy 33:2036
15. Xu B-Q, Wei J-M, Wang H-Y, Sun K-Q, Zhu Q-M (2001) Catal Today 68:217
16. Roh H-S, Potdar HS, Jun K-W (2004) Catal Today 93–95:39
17. Roh H-S, Potdar HS, Jun K-W, Kim J-W, Oh Y-S (2004) Appl Catal A 276:231
18. Trovarelli A, de Leitenburg C, Dolcetti G (1997) Chemtech June:32
19. Kaspar J, Fornasiero P, Graziani M (1999) Catal Today 50:285
20. Rossignol S, Gerard F, Duprez D (1999) J Mater Chem 9:1615
21. de Leitenburg C, Trovarelli A, Lorea JL, Cavani F, Bini G (1996) Appl Catal A 139:161
22. Bekyarova E, Fornasiero P, Kaspar J, Graziani M (1998) Catal Today 45:178
23. Terribile D, Trovarelli A, de Leitenburg C, Primareva A, Dolcetti G (1999) Catal Today 47:133
24. Lercher JA, Bitter JH, Hally W, Niessen W, Seshan K (1996) Stud Surf Sci Catal 101:463
25. Li X, Chang J-S, Park S-E (1999) Chem Lett 1099
26. Li X, Chang J-S, Tian M, Park S-E (2001) Appl Organometal Chem 15:109
27. Roh H-S, Jun K-W, Dong W-S, Park S-E, Baek YS (2001) Catal Lett 74:31
28. Dong W-S, Roh H-S, Jun K-W, Park S-E, Oh Y-S (2002) Appl Catal A 226:63
29. Montoya JA, Romero-Pascual E, Gimon C, Angel PD, Monzon A (2000) Catal Today 63:71
30. Roh H-S, Wang Y, King DL, Platon A, Chin Y-H (2006) Catal Lett 108:15
31. Roh H-S, Platon A, Wang Y, King DL (2006) Catal Lett 110:1
32. Potdar HS, Roh H-S, Jun K-W, Ji M, Liu Z-W (2002) Catal Lett 84:95
33. Jun K-W, Roh H-S, Chary KVR (2007) Catal Surv Asia 11:97
34. Qin D, Lapszewicz J, Jiang X (1996) J Catal 159:140